Bioresource Technology 100 (2009) 6223–6228

Contents lists available at ScienceDirect

Bioresource Technology

journal homepage: www.elsevier.com/locate/biortech

A continuous stirred hydrogen-based polyvinyl chloride membrane biofilm reactor for the treatment of nitrate contaminated drinking water

Siqing Xia [a,*], YanHao Zhang [a,b], FoHua Zhong [a]

[a] State Key Laboratory of Pollution Control and Resource Reuse, College of Environmental Science and Engineering, Tongji University, Shanghai 200092, China
[b] College of Municipal and Environmental Engineering, Shandong Jianzhu University, Jinan 250101, China

ARTICLE INFO

Article history:
Received 27 May 2009
Received in revised form 30 June 2009
Accepted 4 July 2009
Available online 4 August 2009

Keywords:
Hydrogenotrophic denitrification
Membrane biofilm reactor
Polyvinyl chloride membrane
Drinking water

ABSTRACT

A continuous stirred hydrogen-based polyvinyl chloride (PVC) membrane biofilm reactor (MBfR) was investigated to remove nitrate from the drinking water. The reactor was operated over 100 days, and the result showed that the average nitrate denitrification rate of 1.2 g NO_3^-–N/m^2d and the total nitrogen (TN) removal of 95.1% were achieved with the influent nitrate concentration of 50 mg NO_3^-–N/L and the hydrogen pressure of 0.05 MPa. Under the same conditions, the average rate of hydrogen utilization by biofilm was 0.031 mg H_2/cm^2d, which was sufficient to remove 50 mg NO_3^-–N/L from the contaminated water with the effluent nitrate and nitrite concentrations below drinking water limit values. The average hydrogen utilization efficiency was achieved as high as 99.5%. Flux analysis demonstrated that, compared to sulfate reduction, nitrate reduction competed more strongly for hydrogen electron, and obtained more electrons in high influent nitrate loading.

1. Introduction

Removing nitrates and nitrites from drinking water has gained significant attention in recent years due to the risk posed to human health from their contaminated groundwater and surface water. In general, nitrate was mainly from the usage of nitrogen fertilizers (Su and Puls, 2004) and the irrigation with domestic wastewater (Shrimali and Singh, 2001; Soares, 2000). The nitrate concentration in many abstracted waters worldwide now exceeded regulatory standards (WHO and EU, 10 and 11.3 mg NO_3^-–N/L, respectively) (WHO, 2003). These phenomena instigated people to safeguard the risk of methemoglobinemia and cancer induced by nitrosamines, metabolites of nitrate (Bouchard et al., 1992).

The greatest past experience is with abiotic, or physical–chemical treatment methods to remove nitrate and nitrite from drinking water. Abiotic processes include ion exchange (Bae et al., 2002; Boumediene and Achour, 2004), reverse osmosis (Schoeman and Steyn, 2003), and electro-dialysis (Elmidaoui et al., 2002). However, these processes were limited in applications due to high capital and energy costs and subsequent disposal problem of large volumes of waste brine (Shrimali and Singh, 2001).

The biological process that removes nitrate and nitrite is denitrification, which reduces nitrate and nitrite to nitrogen (N_2). Generally, with the low concentration of biodegradable carbon sources in the drinking water, the reduction of nitrate requires addition of electron donor substrates, which include organic carbon sources, such as methanol, ethanol or acetate (belonging to heterotrophic denitrification) (Mohseni-Bandpi and Elliott, 1998; Wang et al., 2009) and a few inorganic electron donors, such as hydrogen and sulfur (belonging to autotrophic denitrification) (Ergas and Reuss, 2001; Koenig and Liu, 1996). While, there are some problems with the heterotrophic denitrification processes, such as bringing carry-over of added organic carbon and microbial biomass to the final effluent.

Autotrophic denitrification using hydrogen as the supplemental donor has been extensively investigated to remove nitrate from polluted drinking water or waste water (Dries et al., 1988; Hasar et al., 2008; Kapoor and Viraraghavan, 1997; Kurt et al., 1987; Lee and Rittmann, 2000). The autohydrogenotrophic denitrifiers are able to respire on NO_3^-–N in the absence of molecular oxygen. Otherwise, hydrogen is cheaper, nontoxic, lower biomass yield, and without a residual.

Generally, there are two ways to transfer hydrogen to the bulk fluid, i.e., sparging the gas or transferring hydrogen to the biofilm through bubbleless gas-permeable membrane (Dries et al., 1988; Kurt et al., 1987; Lee and Rittmann, 2000). With the danger of explosion and low hydrogen utilization rate for the sparging methods, the bubbleless gas-permeable membrane technology has been developed to be a promising way to reduce nitrate, and there are more highlighted advantages for the membranes, such as effective gas transferring and utilization, safe environment for denitrification. To date, a few of bubbleless gas-permeable membranes have been used for hydrogen delivery, such as a double-skinned

* Corresponding author. Tel.: +86 21 65980440; fax: +86 21 65986313.
E-mail addresses: siqingxia@tongji.edu.cn, yanhaozhang@gmail.com (S. Xia).

0960-8524/$ - see front matter © 2009 Elsevier Ltd. All rights reserved.
doi:10.1016/j.biortech.2009.07.002

polyethylene fiber with a dense internal polyurethane layer (1 μm) (Lee and Rittmann, 2000), polypropylene (Terada et al., 2006), silicone-coated reinforced fiberglass fibers (Haugen et al., 2002), silicone-coated ferro-nickel slag (Terada et al., 2006). Although such technology is conceptually promising, there are some challenges to be overcome for the robust reactor development, such as the limit of gas diffusion by the mineral sedimentation and biofilm layer (Visvanathan et al., 2008), deterioration of denitrification performance caused by biofilm sloughing from the membrane (Sawyer and Hermanowicz, 1998). PVC, as a synthetic premise plumbing materials, was extensively used in homes and distribution systems (Cerrato et al., 2006; Heim and Dietrich, 2007), and was safe to drinking water. While PVC fibers were normally used as ultrafiltration membranes in water treatment (Guo et al., 2009; Qiao et al., 2008), they were seldom used as attaching membranes for the biofilm. With the excellent performance of gas diffusing and the cost-effective of membrane fabrication, PVC membrane would be a powerful alternative for hydrogenotrophic denitrification.

This research, which focuses on H_2 as a clean and economical source of electronic donor substrate, investigates the performance of a new PVC hollow fiber membrane biofilm reactor for drinking water denitrification with varied nitrate loading and influent concentrations.

2. Methods

2.1. Membrane biofilm reactor

The experimental set-up of the continuous stirred MBfR used in this study is shown in Fig. 1. A transparent plastic cylinder was used as a hollow fiber membrane reactor, in which two membrane modules were directly submerged in the bulk fluid and gas sealed with the plastic ring and the cap of the reactor (Fig. 1). At the same time, the modules were easily disassembled from the reactor for rinsing or repairing the membranes when the membranes were polluted or damaged. The reactor was 22 cm in height and 6 cm in inner diameter. The system made the feed-media to be mixed well in the biofilm reactor because the stirring power was generated by a magnetic stirrer set in the bottom of the reactor. The hollow fibers were made of PVC with pore size of 0.01 μm, manufactured by Litree Company (Suzhou, China). The outside and inner diameters of the fiber are 0.15 and 0.085 cm, respectively, which provides 633.3 cm^2 of surface area with total 96 hollow fibers (each module consisted of 48 hollow fibers). The total available volume of the reactor system was 560 ml. The void ratio of the working reactor volume (volume of fiber was 23.7 ml) was 95.8%. A single peristaltic pump (Longer BT50-1J, Baoding, PRC) was used to keep a nitrate-medium-feed rate of 1.1 ml/min. Pure H_2 was supplied to the inside hollow fibers through a H_2 gas tank via a metering value.

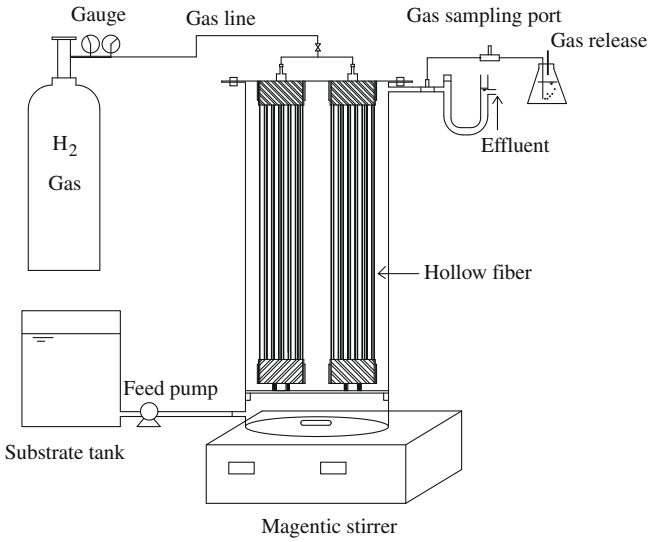

Fig. 1. Schematic of the MBfR.

2.2. Synthetic influent

In present study, the components of synthetic influent for simulating drinking water were KH_2PO_4 (0.128 g/L), Na_2HPO_4 (0.434 g/L), $MgSO_4{\cdot}7H_2O$ (0.2 g/L), $CaCl_2{\cdot}2H_2O$ (0.001 g/L), $FeSO_4{\cdot}7H_2O$ (0.001 g/L), and $NaHCO_3$ (0.252 g/L), and 1 ml trace mineral solution, respectively. Nitrate concentrations ranged from 10 to 50 mg NO_3^-–N/L. The trace mineral solution consisted of: $ZnSO_4{\cdot}7H_2O$ (100 mg/L), $MnCl_2{\cdot}4H_2O$ (30 mg/L), H_3BO_3 (300 mg/L), $CoCl_2{\cdot}6H_2O$ (200 mg/L), $CuCl_2{\cdot}2H_2O$ (10 mg/L), $NiCl_2{\cdot}2H_2O$ (10 mg/L), $Na_2MoO_4{\cdot}2H_2O$ (30 mg/L), and Na_2SeO_3 (30 mg/L), respectively. The feed-media was prepared in a 20 L (available volume) glass bottle, and was purged with N_2 gas to eliminate dissolved O_2 in the influent. $NaNO_3$ and $NaHCO_3$ were used as inorganic nitrogen and carbon sources for the growth of autotrophic microorganisms, respectively. Phosphate buffer (KH_2PO_4 + - Na_2HPO_4) was used to keep initial pH value of the influent around 7.2 and prevent pH from sharp rise during denitrification process.

2.3. Cultivation of microorganisms, start-up and experimental conditions

Start-up of the continuous stirred MBfR began when hydrogen was supplied to the membrane under the hydrogen pressure of 0.02 MPa, and the MBfR was inoculated with mixed-culture biofilm collected from another bioreactor, in which the autohydrogenotrophic denitrifying bacteria had been acclimated for several months. At the beginning of start-up, the reactor had intermittently run for 2 days to establish a biofilm on the membrane surface. Then, under the flow rate of 1.1 ml/min, the performance of continuous stirred MBfR was evaluated over 102 days with varied nitrate loading and influent concentration or hydrogen pressure. The other operation conditions of the reactor were listed in Table 1.

2.4. Analytical method

All the fluid samples collected from the reactor were kept in the refrigerator at 4 °C and analyzed within 2 days. The concentrations of NO_3^-–N, NO_2^-–N, SO_4^{2-} and pH value were analyzed according to Chinese NEPA standard methods (2002). The gas sample in the headspace of the reactor was taken by inserting a gas-tight syringe through the rubber stopper on the gas-sampling port. The gas concentrations were measured by a GC 14-B quipped with a TCD detector (Shimadazu Co.). The liquid phase concentrations of H_2 in the reactor were calculated by H_2 headspace concentrations using Henry's law.

Table 1
Operation conditions of the membrane biofilm reactor.

	Run 1	Run 2	Run 3	Run 4	Run 5
Operation period (day)	1–14	15–28	29–46	47–66	67–102
H_2 pressure (MPa)	0.02	0.02	0.04	0.05	0.05
Influent NO_3^-–N (mg/L)	10	10	20	40	50
Hydraulic retention time (h)			8.5		

2.5. Scanning electron microscopy

A cross section of a new control PVC membrane fiber was obtained by a sterile shaver, and cleaned with distilled water, then dried and coated with Au/Pb in order to enhance the quality of the images. After the preparation, the cross section of the fiber was examined by scanning electron microscope (SEM, XL-30, Philips, Netherlands). Biofilm samples from the reactor were taken during the period of Run 5, and these biofilm samples were checked by SEM using the same methods without the preparation of washing.

3. Results and discussion

3.1. Denitrification performance of continuous stirred MBfR

After the intermittent running of the reactor for 2 days, the continuous influent began. The influent concentrations of nitrate ranged from 10–50 mg N/L (Table 1), while the influent concentrations of sulfate maintained to be around 78 mg SO_4^{2-}/L through the experiments. In Run 1 of the first 14 days, the biofilm was built on the fibers gradually, and nitrate was partially converted to nitrite, but the concentrations of nitrate, nitrite, and sulfate in the effluent dropped gradually to 1.5, 0.6 mg N/L, and 48.5 mg SO_4^{2-}/L, respectively within 14 days (Fig. 2). As shown in Fig. 2, the average total nitrogen (TN) removal efficiency was about 42.2 ± 25.5% in Run 1 and fluctuation of TN was due to the changing of the microorganism community. In fact, the autohydrogenotrophic denitrifier in Run 1 were in the cultivation and enrichment stage.

After 14 days, the experiment went into Run 2, which was actually a continuation of the steady state of Run 1. For Runs 3 and 4, the hydrogen pressures were adjusted to 0.04, and 0.05 MPa, respectively to enhance the activity of hydrogenotrophic denitrifying bacteria. The system achieved excellent running performance, and the average removal efficiencies of nitrate in the three running stages were 92.8%, 98.5%, and 99.5%, respectively. Although the influent nitrate concentration increased gradually from 10 to 40 mg N/L, the average of residual nitrate concentrations in the effluent decreased progressively from 0.7 to 0.2 mg N/L, and the effluent concentrations of nitrite were hardly detected in the three running stages.

During Run 5, the average concentrations of nitrate, nitrite, and sulfate in the effluent increased to 2.2 ± 2.0 mg N/L, 0.4 ± 0.3 mg N/L, and 46.5 ± 8.7 mg SO_4^{2-}/L, respectively. Especially, the nitrite concentrations in the effluent were detected up to 0.9 mg N/L in the previous period of Run 5, i.e., the nitrite accumulation occurred, which suggested that the reactor was operated near its maximum nitrate loading capacity, and the bacterial cells preferentially utilized nitrate as the sink for electrons over nitrite (Lee and Rittmann, 2002). Therefore, the effluent equality in hydrogenotrophic denitrification processes must be closely monitored to ensure that the nitrite concentration does not exceed regulatory levels (WHO, 1 mg N/L).

Fig. 3 shows the changes of influent nitrate loading rate, volumetric denitrification rate and TN removal in the continuous experiment. From Run 2 to Run 5, the average nitrate volumetric loading rate increased from 29.1 to 141.7 g N/m^3d, and the average volumetric denitrification rates were 27.0, 55.3, 114.0, and 136.0 g N/m^3d, respectively, which corresponded to average surface denitrification rates of 0.24, 0.49, 1.01, and 1.20 g N/m^2d, respectively. Meanwhile, the average TN removal rate reached 92.8%, 98.4%, 98.9%, and 94.4% in Runs 2–5, respectively. A nearly complete removal of influent nitrate (40 mg N/L) was attained by the continuous stirred MBfR at 114.0 g N/m^3d. The results were favorably compared to that reported by Lee and Rittmann (2000) of 1.0 g N/m^2d and were close to the result by Shin et al. (2008) of 1.4 g N/m^2d in their work with hydrogenotrophic denitrification in hollow fiber membrane bioreactors. Terada et al. (2006) had reported a high surface denitrification rate of 3.53–6.58 g N/m^2d by hydrogen-based silicone membrane biofilm reactor which employed fibrous ferro-nickel slag as a bacterial support; however, the membrane built-up was complicated and the hydrogen utilization efficiency was about 40%, which had a potential of having explosive air.

The outer morphologies for cross section of the new control hollow fiber and biofilm surface from the reactor are demonstrated in the SEM images. The cross section of the control fiber showed the mesh structure of the PVC hollow fiber wall, which consists of pores about 80 μm long and 20 μm wide. This structure makes the fiber have enough tensile strength and flexibility to be operated in water or wastewater treatment for a long period. However, the fiber surface is a flat surface, the micro-pores of 0.01 μm could not be seen clearly because of special process for film manufacturing. Throughout the duration of the experiments the membrane had not been broken once. As shown in the SEM image of biofilm surface, the biofilm taken from the reactor visually consisted of individual rod-shape bacteria about 0.3 μm in diameter and 2 μm long (Chung et al., 2006a).

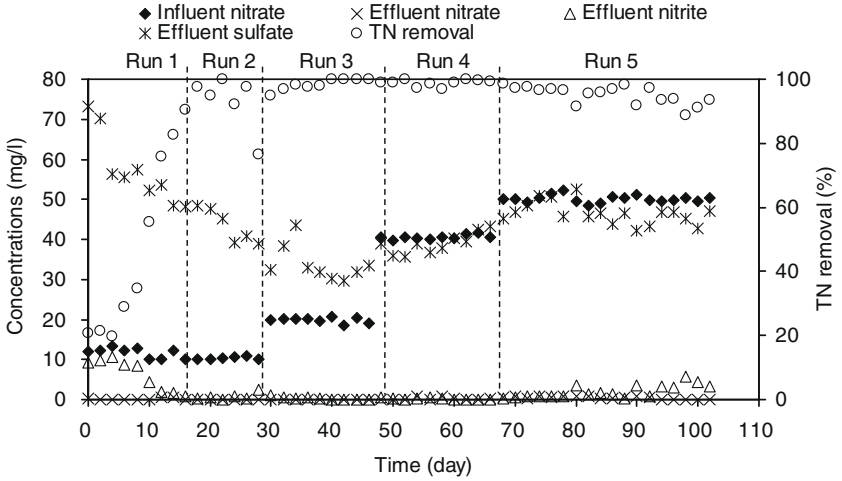

Fig. 2. The nitrate, nitrite, sulfate and TN removal in the continuous experiments.

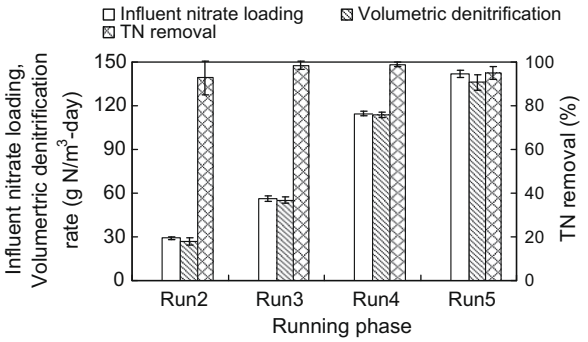

Fig. 3. Influent nitrate loading, volumetric denitrification rate and TN removal in the experiment. Error bars represent the standard deviation between continuous samples during one running phase.

3.2. Flux analysis

Table 2 summarized the average values of substrate fluxes and electron-equivalent fluxes for all the electron acceptors, along with the percentage distribution of each flux. Compared to Run 1, both of the fluxes of nitrate and sulfate in Run 2 were increased almost two times. The results suggested that the biofilm was on the state of growing period in Run 1 and the H_2 supply at 0.02 MPa was excessive. After 14 days, the biofilm developed into a steady state, where the TN removal and sulfate removal achieved 82.6% and 38.2%, respectively (Fig. 2). The distributions of electron-equivalent flux for nitrate and sulfate did not change much from Run 1 to Run 2, while, the electron-equivalent flux for nitrate was little more than that for sulfate in the two running stages.

From Run 2 to Run 3, the flux of nitrate increased almost two times, as the influent nitrate concentration was increased to 20 mg N/L and hydrogen pressure increased to 0.04 MPa. The nitrate reduced completely in the steady state in Run 3, but the flux of sulfate had few increments of 0.24 g SO_4^{2-}/m^2d, and the average sulfate removal in Run 3 was 56.4%. The result was consistent to Terada et al. (2006), they reported approximately 50% of sulfate was reduced by sulfate reduction bacteria (SRB) when hydrogen pressure increased to 0.05 MPa. Thereafter, with the influent nitrate loading increasing, the fluxes of nitrate continued to increase proportionally, however, the sulfate fluxes declined gradually, from 1.09 to 0.75 g SO_4^{2-}/m^2d. This is an evidence of competition between nitrate and sulfate reduction for electrons at a fixed availability of H_2 (0.05 MPa).

As shown in Table 2, the flux of electron to nitrate reduction was strongly improved as influent nitrate loading increased. The nitrate reduction was a lager consumer of electrons in all the running stages, especially in the highest influent nitrate loading in Run 5, e.g. the electron-equivalent flux of nitrate accounted for 87.5% of the total electron flux. However, the flux of electron to sulfate reduction declined gradually with the same influent sulfate loading. On the one hand, nitrate reduction competed more strongly for H_2. On the other hand, as the H_2 pressure increased from 0.02 MPa in Run 1 to 0.05 MPa in Run 4, the sulfate flux normalized by its effluent concentration increased from 0.008 to 0.025 m/d (data not shown). This demonstrated that sulfate reduction strongly depended on H_2 availability (Chung et al., 2006b).

3.3. Hydrogen utilization

In the experiments, hydrogen consumption was mainly attributed to nitrate and sulfate reduction. According to Lee and Rittmann (2002), with analyzing the hydrogen utilization of the system, the mass balances of hydrogen, nitrate, nitrite, and sulfate in the autohydrogenotrophic biofilm were built under the fundamental assumptions. The assumptions are: the substrate utilized by the suspended biomass is ignored and biomass is not included in the mass balances. According to the stoichiometry of hydrogen utilization for denitrification and sulfate reduction (Lee and Rittmann, 2002; Chung et al., 2006b), the sum of hydrogen consumption rates during denitrification and sulfate reduction by the biofilm ($R_{H,B}$, mg H_2/cm^3d) can be described by Eq. (1), and the hydrogen flux ($J_{H,T}$, mg H_2/cm^2d) can be described by Eq. (2).

$$R_{H,B}V = \alpha_{H,3}Q(S_{3,i} - S_{3,o}) + \alpha_{H,2}\alpha_{2,3}Q(S_{3,i} - S_{3,o}) + \alpha_{H,4}Q(S_{4,i} - S_{4,o}) - \alpha_{H,2}QS_{2,o} \quad (1)$$

$$J_{H,T}A_B = R_{H,B}V + QS_{H,o} \quad (2)$$

where $R_{H,B}$ is the rate of hydrogen utilization by the biofilm (mg H_2/cm^3d). $\alpha_{H,3}$ is the stoichiometric consumption ratio of hydrogen to nitrate during nitrate reduction (mg H_2/mg N), $\alpha_{H,2}$ is the stoichiometric consumption ratio of hydrogen to nitrite during nitrite reduction to N_2 gas (mg H_2/mg N), and $\alpha_{H,4}$ is the stoichiometric consumption ratio of hydrogen to sulfate during sulfate reduction to sulfide (mg H_2/mg SO_4^{2-}). Based on the stoichiometric reactions of hydrogen utilization for denitrification and sulfate reduction (Lee and Rittmann, 2002; Chung et al., 2006b) and Eq. (1), $\alpha_{H,3}$, $\alpha_{H,2}$, and $\alpha_{H,4}$ are 0.143, 0.214 mg H_2/mg N, and 0.083 mg H_2/mg SO_4^{2-}, respectively. $\alpha_{2,3}$ is the stoichiometric coefficient for the production of nitrite from nitrate to nitrite, which is equal to 1 mg N/mg N. A_B is the biofilm surface area (cm^2), Q is the influent flow rate of the reactor system (l/d), V is the volume of the reactor (cm^3). $S_{3,i}$ and $S_{3,o}$ are the nitrate concentrations in the influent and the effluent respectively (mg N/L); $S_{4,i}$ and $S_{4,o}$ are the sulfate con-

Table 2
Electronic-equivalent fluxes for sulfate and nitrate.

Period	Denitrification rate or substrate flux[a]		Electron-equivalent flux (eq/m^2d)			Distribution of electron-equivalent fluxes (%)	
	Nitrate (g/m^2d)	Sulfate (g SO_4^{2-}/m^2d)	Nitrate[b]	Sulfate[c]	Sum up of the fluxes	Nitrate	Sulfate
Run 1	0.13	0.47	0.05	0.04	0.08	54.1	45.9
Run 2	0.24	0.85	0.09	0.07	0.15	55.3	44.7
Run 3	0.49	1.09	0.17	0.09	0.26	66.2	33.8
Run 4	1.01	0.96	0.36	0.08	0.44	82.2	17.8
Run 5	1.20	0.75	0.43	0.06	0.49	87.5	12.5

[a] Calculated by $J_{substrate} = \frac{\text{Influent flow rate}(Q)\times\text{removed substrate}(\Delta S)}{\text{Area of biofilm surface}(A_B)}$, where Q is in m^3/d, ΔS is in g-substrate (NO_3^-–N or SO_4^{2-})/m^3, A_B is in m^2, and J is in g-NO_3^-–N/m^2d or g-SO_4^{2-}/m^2d.

[b] Calculated by $J_{e-NO_3^-} = \frac{\text{Influent flow rate}(Q)\times\text{removed } NO_3^-\text{–N}(\Delta S)}{\text{Area of biofilm surface}(A_B)\times EW_{Nitrate}}$, where Q is in m^3/d, ΔS is in g-NO_3^-–N/m^3, A_B is in m^2, $EW_{Nitrate}$ is 14 in g-NO_3^-–N/5, e^- equivalent for reduction of nitrate to nitrogen gas, and J is in g-NO_3^-–N/m^2d. We assume five electrons per mole for nitrate reduction to nitrogen gas.

[c] Calculated by $J_{e-NO_3^-} = \frac{\text{Influent flow rate}(Q)\times\text{removed } SO_4^{2-}(\Delta S)}{\text{Area of biofilm surface}(A_B)\times EW_{Sulfate}}$, where Q is in m^3/d, ΔS is in g-SO_4^{2-}/m^3, A_B is in m^2, $EW_{Sulfate}$ is 96 in g-NO_3^-–N/8, e^- equivalent for reduction of sulfate to sulfide, and J is in g-SO_4^{2-}/m^2d. We assume eight electrons per mole for sulfate reduction to sulfide, for seen $SO_4^{2-} + 4H_2 + 1.5H^+ \rightarrow 0.5H_2S + 0.5HS^- + 4H_2O$ (Chung et al., 2006b).

centrations in the influent and the effluent respectively (mg SO_4^{2-}/L); $S_{H,o}$ is hydrogen concentration in the effluent (mg H_2/L). Then, the rate of hydrogen utilization by the biofilm, the hydrogen concentration in the effluent, and the hydrogen flux in the experiment are demonstrated in Fig. 4.

The hydrogen concentrations in the effluent dropped and the rates of hydrogen utilization increased with the time or with the influent nitrate loading increasing. In Run 5, the maximum average rate of hydrogen utilization by biofilm was 0.055 mg H_2/cm^3d, which corresponded to 0.031 mg H_2/cm^2d of average hydrogen flux. The results were consistent to that reported by Lee and Rittmann (2002), and this hydrogen flux was sufficient to remove 50 mg NO_3^-–N/L from the contaminated water with lower nitrate and nitrite concentrations below regulatory levels. Fig. 4 also illustrates the changes of effluent hydrogen concentration in different running stages. The effluent hydrogen concentration decreased as the nitrate loading increased and then leveled off at the last running stages, averaged 99 ± 29 μg/L in Run 5. This result indicated that the nitrate loading limitation for autohydrogenotrophic denitrification was transited to hydrogen limitation at the stage of effluent hydrogen concentration leveling off.

The % unutilized hydrogen was calculated as the ratio of H_2 leaving in the effluent divided by the H_2 used for nitrate reduction, nitrite reduction, sulfate reduction, and loss to the effluent, as shown in Eq. (3). Based on the % unutilized hydrogen in the experiment, the % utilized hydrogen could be calculated correspondingly. With the reactor running, the average hydrogen utilization efficiencies increased gradually. The lower hydrogen utilization efficiency in Run 1 of 75.9 ± 11.3% could be explained by the fact that the microorganisms in the biofilm were in the state of acclimating periods and the autohydrogenotrophic denitrification denitrifiers were not the dominant bacteria. With the denitrification efficiency increasing, the biofilm developed into a steady state in Run 2, the average hydrogen utilization efficiencies in Runs 2–5 increased, for seen 88.3%, 93.6%, 99.3%, and 99.5%, respectively. The results were favorably compared to Ergas and Reuss (2001) of 40% hydrogen utilization efficiency using hollow fiber membrane without gas-ended, and Terada et al. (2006) of also around 40% hydrogen utilization efficiency with silicone-coated ferro-nickel slag, and close to Lee and Rittmann (2002) of 99.9% hydrogen utilization efficiency using PE membrane in their works with autohydrogenotrophic denitrification. The high hydrogen utilization efficiencies were mainly attributed to the counter-diffusion transfer of H_2 directly in the biofilm and the excellent performance of micro-pore PVC membrane. Hydrogen is supplied through a gas-permeable membrane, while NO_3^-–N comes from the bulk, in turn, the other side of hydrogen supply. Theoretically, hydrogen and NO_3^-–N are never present at the same location in their maximum concentrations for the membrane biofilm as reported by Rittmann (2002).

$$\%H_2\text{unutilized} = 100\% \times \frac{S_{H,o}}{0.143(S_{3,i}-S_{3,o})+0.214(S_{3,i}-S_{3,o}-S_{2,o})+0.083(S_{4,i}-S_{4,o})+S_{H,o}} \quad (3)$$

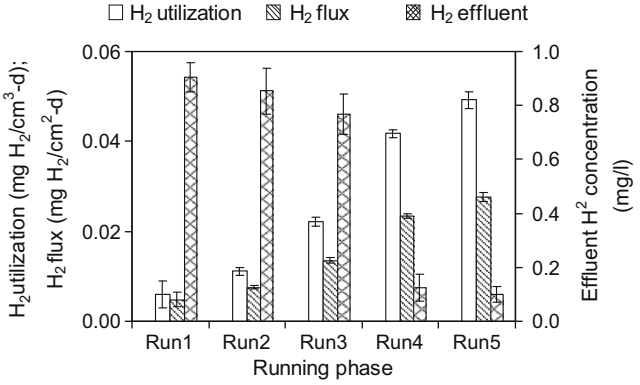

Fig. 4. Average rate of hydrogen utilization by the biofilm, average hydrogen concentration in the effluent, and average hydrogen flux at different experimental periods. Error bars represent the standard deviation between continuous samples during one running phase.

4. Conclusion

The present study indicted that the continuous stirred PVC MBfR can be used effectively for nitrate remove in drinking water. Under the conditions of influent nitrate concentration 50 mg N/L and hydrogen pressure 0.05 MPa, the average denitrification rate achieved was 1.20 g NO_3^-–N/m^2d. The rate and efficiency of hydrogen utilization by the biofilm averaged 0.031 mg H_2/cm^2d, and 99.5%, respectively. The fluxes analysis showed that nitrate reduction could consume more electrons in high influent nitrate loading than that in low influent nitrate loading, and nitrate reduction was not significantly influenced by sulfate reduction.

Acknowledgements

The authors thank to the Programs of Internationally Scientific Cooperation (2007DFB90280, 2007DFR90050) and Special Program of World Exposition (07DZ05814) for providing the financial support.

References

Bae, B.U., Jung, Y.H., Han, W.W., Shin, H.S., 2002. Improved brine recycling during nitrate removal using ion exchange. Water Res. 36, 3330–3340.
Bouchard, D.C., Williams, M.K., Surampalli, R.Y., 1992. Nitrate contamination of groundwater: sources and potential health effects. Am. Water Works Assoc. 84, 85–90.
Boumediene, M., Achour, D., 2004. Denitrification of the underground waters by specific resin exchange of ion. Desalination 168, 187–194.
Cerrato, J.M., Reyes, L.P., Alvarado, C.N., Dietrich, A.M., 2006. Effect of PVC and iron materials on Mn(II) deposition in drinking water distribution systems. Water Res. 40, 2720–2726.
Chinese NEPA, 2002. Water and Wastewater Monitoring Methods, fourth ed. Chinese Environmental Science Publishing House, Beijing, China.
Chung, J., Li, X.H., Rittmann, B.E., 2006a. Bio-reduction of arsenate using a hydrogen-based membrane biofilm reactor. Chemosphere 65, 24–34.
Chung, J., Nerenberg, R., Rittmann, B.E., 2006b. Bioreduction of selenate using a hydrogen-based membrane biofilm reactor. Environ. Sci. Technol. 40, 1664–1671.
Dries, D., Liessens, J., Verstraete, W., Stevens, P., De Vos, P., De Ley, J., 1988. Nitrate removal from drinking water by means of hydrogenotrophic denitrifiers in a polyurethane carrier reactor. Water Supply 6, 181–192.
Elmidaoui, A., Elhannouni, F., Tahaiki, M., Taky, M., Chay, L., Mohamed, A.S., Echihabi, L., Hafsi, M., 2002. Optimization of nitrate removal operation from groundwater by electrodialysis. Sep. Purif. Technol. 29, 235–244.
Ergas, S.J., Reuss, A.F., 2001. Hydrogenotrophic denitrification of drinking water using a hollow fibre membrane bioreactor. Water Supply: Res. Technol. AQUA 50, 161–171.
Guo, X., Zhang, Z., Fang, L., Su, L., 2009. Study on ultrafiltration for surface water by a polyvinyl chloride hollow fiber membrane. Desalination 238, 183–191.
Hasar, H., Xia, S.Q., Ahn, C.H., Rittmann, B.E., 2008. Simultaneous removal of organic matter and nitrogen compounds by an aerobic/anoxic membrane biofilm reactor. Water Res. 42, 4109–4116.
Haugen, K.S., Semmens, M.J., Novak, P.J., 2002. A novel in situ technology for the treatment of nitrate contaminated groundwater. Water Res. 36, 3497–3506.
Heim, T.H., Dietrich, A.M., 2007. Sensory aspects and water quality impacts of chlorinated and chloraminated drinking water in contact with HDPE and cPVC pipe. Water Res. 41, 757–764.
Kapoor, A., Viraraghavan, T., 1997. Nitrate removal from drinking water – review. J. Environ. Eng.-ASCE 123, 371–380.
Koenig, A., Liu, L.H., 1996. Autotrophic denitrification of landfill leachate using elemental sulfur. Water Sci. Technol. 34, 469–476.
Kurt, M., Dunn, J., Bourne, J.R., 1987. Biological denitrification of drinking water using autotrophic organisms with H_2 in a fluidized-bed biofilm reactor. Biotechnol. Bioeng. 29, 493–501.

Lee, K.C., Rittmann, B.E., 2000. A novel hollow fiber membrane biofilm reactor for autohydrogenotrophic denitrification of drinking water. Water Sci. Technol. 41, 219–226.
Lee, K.C., Rittmann, B.E., 2002. Applying a novel autohydrogenotrophic hollow-fiber membrane biofilm reactor for denitrification of drinking water. Water Res. 36, 2040–2052.
Mohseni-Bandpi, A., Elliott, D.J., 1998. Groundwater denitrification with alternative carbon sources. Water Sci. Technol. 38, 237–243.
Qiao, X., Zhang, Z., Yu, J., Ye, X., 2008. Performance characteristics of a hybrid membrane pilot-scale plant for oilfield-produced wastewater. Desalination 225, 113–122.
Rittmann, B.E., 2002. Hydrogen-based membrane-biofilm reactor solves oxidized contaminant problems. Membr. Technol., 6–10.
Sawyer, L.K., Hermanowicz, S.W., 1998. Detachment of biofilm bacteria due to variations in nutrient supply. Water Sci. Technol. 37, 211–214.
Schoeman, J.J., Steyn, A., 2003. Nitrate removal with reverse osmosis in a rural area in South Africa. Desalination 155, 15–26.
Shin, J.H., Sang, B.I., Chung, Y.C., Choung, Y.K., 2008. A novel CSTR-type of hollow fiber membrane biofilm reactor for consecutive nitrification and denitrification. Desalination 221, 526–533.
Shrimali, M., Singh, K.P., 2001. New methods of nitrate removal from water. Environ. Pollut. 112, 351–359.
Soares, M.I.M., 2000. Biological denitrification of groundwater. Water, Air, Soil Pollut. 123, 183–193.
Su, C.M., Puls, R.W., 2004. Nitrate reduction by zerovalent iron: effects of formate, oxalate, citrate, chloride, sulfate, borate, and phosphate. Environ. Sci. Technol. 38, 2715–2720.
Terada, A., Kaku, S., Matsumoto, S., Tsuneda, S., 2006. Rapid autohydrogenotrophic denitrification by a membrane biofilm reactor equipped with a fibrous support around a gas-permeable membrane. Biochem. Eng. J. 31, 84–91.
Visvanathan, C., Hung, N.Q., Jegatheesan, V., 2008. Hydrogenotrophic denitrification of synthetic aquaculture wastewater using membrane bioreactor. Process Biochem. 43, 673–682.
Wang, Q.H., Feng, C.P., Zhao, Y.X., Hao, C.B., 2009. Denitrification of nitrate contaminated groundwater with a fiber-based biofilm reactor. Bioresour. Technol. 100, 2223–2227.
WHO, 2003. Guidelines for Drinking Water Quality, third ed. Geneva.